Virtual Power Plant Control for Large Residential Communities using HVAC Systems for Energy Storage

Huangjie Gong, *Student Member, IEEE*, Evan S. Jones, *Student Member, IEEE*, Rosemary E. Alden, *Student Member, IEEE*, Andrew G. Frye, Donald Colliver, and Dan M. Ionel, *Fellow, IEEE*

***Abstract*—Heating, ventilation, and air-conditioning (HVAC) systems use the most electricity of any household appliance in residential communities. HVAC system modeling facilitates the study of demand response (DR) at both the residential and power system levels. In this paper, the equivalent thermal model of a reference house is proposed. Parameters for the reference house were determined based on the systematic study of experimental data obtained from fully instrumented field demonstrators. Energy storage capacity of HVAC systems is calculated and an equivalent state-of-charge (SOC) is defined. The uniformity between HVAC systems and battery energy storage systems (BESS) is demonstrated by DR control. The aggregated HVAC load model is based on the reference house and considers a realistic distribution of HVAC parameters derived from one of the largest smart grid field demonstrators in rural America. A sequential DR scheme as part of a Virtual Power Plant (VPP) control is proposed to reduce both ramping rate and peak power at the aggregated level, while maintaining human comfort according to ASHRAE standards.**

***Index Terms*—Heating, Ventilation, and Air-conditioning (HVAC), Battery Energy Storage System (BESS), Home Energy Management (HEM), Demand Response (DR), Equivalent Thermal Model, Aggregated, Grey Box, Virtual Power Plant (VPP), Smart Home, Smart Grids, Equivalent Energy Storage, American Society of Heating, Refrigerating and Air-Conditioning Engineers (ASHRAE).**

I. Introduction

Heating, ventilation, and air-conditioning (HVAC) systems use the highest percentage of energy within typical residences [1]. They dominate the house energy usage and contribute the most to the peak power demand at the aggregated level. To accommodate large fluctuations in demand over the course of a day, expensive infrastructure must be installed to meet the maximum demand. This leads to extra cost and a need for optimized control to reduce the peak power.

Utilizing HVAC systems as demand response (DR) devices has great opportunity to yield significant energy savings, especially at an aggregated level. To properly study the simulated implementation of HVAC DR schemes, a valid model of HVAC energy use is required. A grey-box resistance-capacitance (RC) model provides accurate results for the indoor temperature with proper values for R and C [2], [3]. Aggregated modeling for a community of air conditioning loads has been proven effective for the study of large-scale DR implementation [4]. Commercial HVAC system modeling employs statistical methods that are also highly accurate [5].

The DR studies with residential-level HVAC models, however, are more recent and have yet to reach this degree of confidence due to the strong link among HVAC energy use, random user behavior, and external weather conditions. The effect of weather induces more variation in energy and is more difficult to capture at the residential level. Current research proposes various methods to develop residential HVAC energy models, such as power-temperature modeling through disaggregation of smart meter data [6], or employing whole building energy simulators like EnergyPlus [7], or eQUEST [8].

Studies have provided multiple demonstrations for the effectiveness of HVAC systems as DR devices through control or price-based schemes [9]. A study in which indoor temperature of an individual simulated building was controlled based on electricity retail prices found that heating and cooling energy use was reduced by 12% and 21% for the coldest and hottest months, respectively [10]. A bonus-based DR approach that employs Stackelberg game theory to reduce mismatch between residential energy use and renewable generation also yielded significant results with a reduced deviation ranging from about 32% to 43% [11]. A bi-level optimal control study including residential HVAC systems resulted in as much as 22% in energy savings [12].

To ensure adequate thermal comfort, the HVAC control follows Standard 55 of the American Society of Heating, Refrigerating and Air-Conditioning Engineers (ASHRAE), in terms of external and internal temperature, relative humidity, individual metabolic rate, etc. [13]. The ASHRAE Standards quantify the comfort of the space using a numerical scale called the Predicted Mean Vote (PMV) that was derived from survey results where participants ranked their comfort from -3, very cold, to 3, very hot. This allows for an association between a range of environmental conditions to a comfortable status within a home that can be calculated as a PMV between -0.5 and 0.5, which may be used to control heating and cooling systems without affecting thermal comfort.

HVAC systems are widely perceived as solely energy-

H. Gong, E. S. Jones, R. E. Alden, and D. M. Ionel are with the SPARK Laboratory, Department of Electrical and Computer Engineering, University of Kentucky, Lexington, KY, USA (e-mail: {huangjie.gong, sevanjones, rosemary.alden}@uky.edu, dan.ionel@ieee.org).
A. G. Frye is with Tennessee Valley Authority, Knoxville, TN, USA (e-mails: agfrye@tva.gov).
D. Colliver is with Biosystems and Ag Engineering Department, University of Kentucky, Lexington, KY, USA (e-mails: dcolliver@uky.edu).

consuming in the power grid. This view is being re-assessed in the field of home energy management (HEM) as recent research from the Oak Ridge National Laboratory (ORNL) demonstrates that the HVAC system can be regarded as an equivalent energy storage device and be conveniently controlled by a similar charging/discharging procedure [14]. For example, a commercial building with multiple zones can be modeled to operate as an equivalent energy storage device and can be controlled by adjusting zonal airflow rates [15]. As claimed in [16], the round trip efficiency of the HVAC-based equivalent energy storage can be near 100%.

Electrical energy storage systems cab be divided into three categories: electrochemical, mechanical, and ultracapacitors [17]. A deferrable load can be redefined as an energy storage device by three integral properties: "the volume of energy that can be stored, the rate at which energy can be absorbed, and the rate at which energy can be released" [18]. This uniformity enables a single HEM strategy across electric energy storage devices and deferrable energy loads [19], [20].

A research gap remains as most HVAC system models require parameters that are challenging to acquire [21]. It becomes increasingly difficult for aggregated HVAC load modeling considering additional parameters for the multiple buildings. Some alternative methods for aggregated HVAC load modeling may only monitor the average room temperature for multiple buildings, ignoring the thermal comfort of individual users [22], [23].

This paper is a substantially expanded follow up of a previous conference paper by the same research group, which proposed the thermal model of a reference house, and derived the parameters from experimental data provided by a robotic house field demonstration conducted by the Tennessee Valley Authority (TVA) in Knox County, TN [24]. In the conference paper, the equivalent thermal resistance of the reference house was analyzed. The aggregated HVAC power for 10,000 houses was modeled and validated against the experimental data from the Smart Energy Technologies (SET) project in Glasgow, KY, one of the largest smart grid demonstrators in rural USA [25].

Based on the previous conference paper, this work justified the thermostat set point of the HVAC systems to ensure human comfort according to ASHRAE standards. A centralized sequential DR control method for the reduction of the ramping rate and peak power was elaborated in this work. Additionally, the comparability between the HVAC system and a typical battery energy storage system (BESS) was studied and demonstrated. Cases for different hot days, and for one day with different residence participation were studied.

The major contributions of the paper include: (1) modeling of a HVAC system with minimum parameters derived from experimental data; (2) an aggregation technique for large communities based on realistic distribution of HVAC parameters and loads; (3) development of the equivalent energy storage model for the HVAC system; (4) proposal of sequential control for the HVAC systems in a large community; (5) justification of the consumer comfort based on the ASHRAE standards.

The arrangement of the paper is as follows. The experimental results and the derivation of the parameters for the house thermal model are introduced in Section II. The HVAC as equivalent energy storage is analyzed in Section III. In Section IV, the aggregated HVAC load is modeled. The proposed sequential DR control and the simulation results are presented and discussed in Sections V and VI, respectively. The conclusions are drawn in Section VII.

Fig. 1. The reference house (a). TVA robotic devices are controlled by computer programs to mimic realistic human behavior. Also shown is a shower emulator (b), automated dryer and washer (c), and a refrigerator with programmed arms (d) that activate according to automatic schedules.

II. Experimental Results and Derivation of House Thermal Model Parameters

Beginning in 2008, TVA funded and managed a robotic house project with technical support from the ORNL. The robotic houses were constructed in a suburb of Knox County, TN in which the habitation of a family was physically emulated (Fig. 1). This project developed an analytical base for energy optimization and new technology implementation at the individual house level. A different initiative, the SET project based in Glasgow, KY, provided a testbed for the optimization of power flow at the community level. In the TVA robotic house, energy usage for different components, including the HVAC, was measured on an hourly basis. The experimental data from SET had a 15-minute resolution.

The equivalent model that represents a typical residence, which was defined by parameters such as thermal envelope area, thermal resistance, thermal capacitance, and heat transfer rate was derived from the TVA robotic house experimental data. The thermal envelope area is the only independent variable for the equivalent model. Other parameters for the equivalent thermal model were calculated using the thermal envelope area and coefficients, as follows:

TABLE I
PARAMETERS FOR THE THERMAL MODEL OF THE REFERENCE HOUSE

Parameter	Value
Thermal envelope area A_r	354 m^2
Coefficient of thermal resistance c_R	350 $^\circ C \cdot m^2/kW$
Coefficient of thermal capacitance c_C	0.011 $kWh/(^\circ C \cdot m^2)$
Coefficient of heat transfer rate c_P	0.040 kW/m^2

$$R = \frac{c_R}{A_r}, \quad C = c_C \cdot A_r, \quad P_H = c_P \cdot A_r, \tag{1}$$

where R, is the thermal resistance; C, the thermal capacitance; and P_H, heat transfer rate. The other parameters are specified in Table I.

The heat transfer function of the residential thermal model is described as follows:

$$C\frac{\mathrm{d}\theta_I(t)}{\mathrm{d}t} = \frac{1}{R}\Big(\theta_O(t) - \theta_I(t)\Big) - S(t) \cdot P_H, \tag{2}$$

where θ_I is the indoor temperature; θ_O, the outdoor temperature; S, the ON/OFF status of HVAC, defined as:

$$S(t) = \begin{cases} 0, & \text{if } S(t-1) = 1 \ \& \ \theta_I(t) \le \theta_L(t) \\ 1, & \text{if } S(t-1) = 0 \ \& \ \theta_I(t) \ge \theta_H(t) \\ S(t-1), & \text{otherwise,} \end{cases} \tag{3}$$

where θ_L and θ_H are the lower and upper band of the thermostat set point, of 70F and 74F, respectively for the TVA robotic house.

The data provided by the robotic house has a resolution of 1-hour. Data from July of 2010 was used for the calculation of the parameters and the validation of the equivalent thermal model. The thermal resistance R was calculated assuming that the indoor temperature rate of change remained constant for every two consecutive hours, i.e., $\mathrm{d}\theta_\mathrm{I}(\mathrm{t}) = 0$ in (2) through the whole month. Only hourly data for 12:00-16:00 of each day in July was used to estimate the coefficient of thermal resistance c_R, as during these times it is likely that the HVAC would be working, i.e., $S(t) = 1$ in (2). The calculated coefficient of the equivalent resistance based on the robotic house data is shown in Fig. 2. The solar heat gain as well as the latent and appliance heat gains were lumped together in the thermal resistance term.

The HVAC system for the reference house was modeled with fixed parameters (Table I). The envelope area was calculated according to the floor plan. The coefficient of thermal resistance c_R was selected according to its relationship to outdoor temperature and justified with a confidence interval (Fig. 2). The c_C and c_P were adjusted based on the envelope area and recommended values [26]. With a cooling capacity of 4 tons and a Seasonal Energy Efficiency Ratio (SEER) of 13.5, the HVAC system had a constant input electrical power of approximately 3.6kW when it was ON (Fig. 3).

The experimental data from July, 2010, which was retrieved from the robotic house project supported by TVA and ORNL,

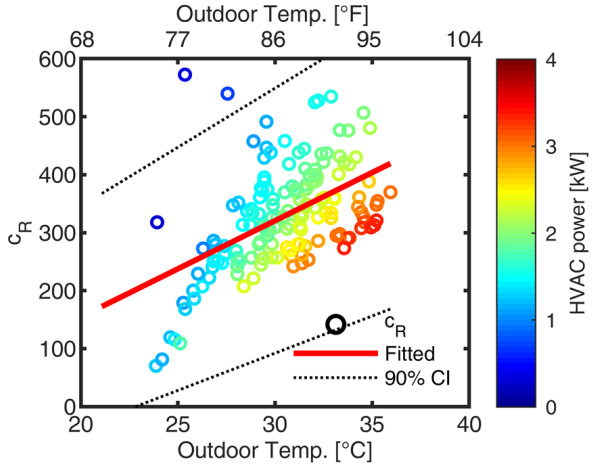

Fig. 2. Analysis of the c_R equivalent thermal resistance coefficient for the reference house. Data corresponds to 5 hours during the time interval of direct interest for DR studies of each day in July 2010. Data was fitted with a 90% confidence interval, and only 2 points were outside the bounds.

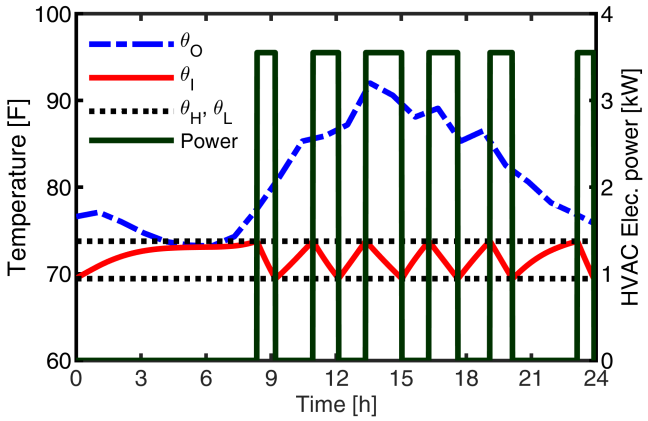

Fig. 3. The daily simulation example of the HVAC system for the reference house. With a cooling capacity of 4 tons and a SEER of 13.5, the HVAC has approximately 3.6kW of constant electric power during operation.

was used for the validation of the residential thermal model. For most of the days in Fig. 4, the outdoor temperature was high in the afternoon. The daily HVAC electricity usage for the experimental and simulated data are compared and presented in Fig. 5. Apart from the first few days and the last day when the outside temperature was relatively low, the simulation had highly satisfactory results.

Further study found that the proposed residential thermal model resulted in lower electricity daily usage for the HVAC when the outdoor temperature was both low and measured on an hourly basis. This occurred due to the cessation of HVAC operation during higher temperatures that were artificially reduced by the hourly temperature measurements. For example, if the thermostat set point was 75F and the outdoor temperature was 70F for half the hour and 80F for the other half, the experimental data would have the HVAC ON for only the half hour. However, the averaged hourly based temperature data

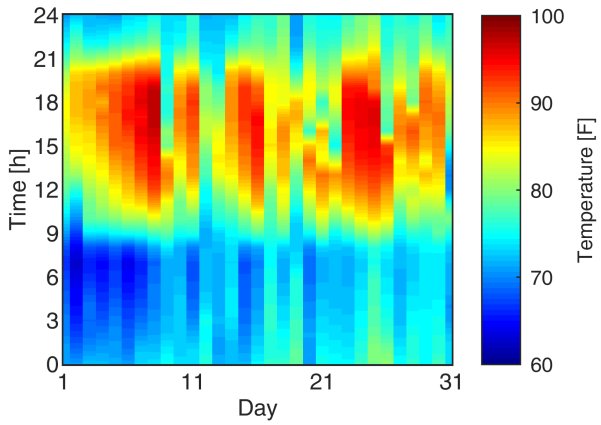

Fig. 4. The outdoor temperature in July 2010 Knox County, TN. The temperature of this month was used for the calibration of the residential thermal model.

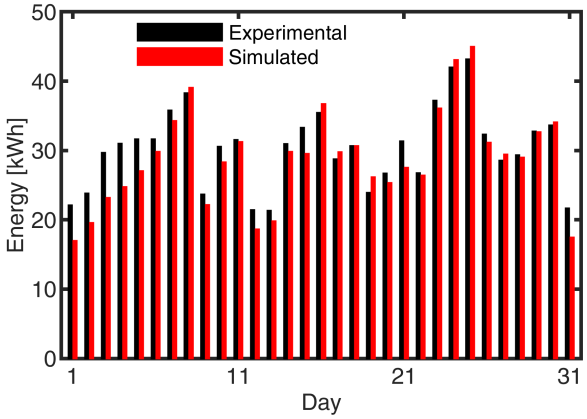

Fig. 5. The daily HVAC electricity usage of the TVA robotic house in July, 2010. The simulation results were calculated using the proposed residential thermal model and parameters. The experimental data was retrieved from the robotic house project supported by TVA and ORNL.

would be 75F, under which case the modeled HVAC would be OFF the entire hour.

III. HVAC System as Equivalent Energy Storage

The HVAC system is described as equivalent energy storage, and its equivalent SOC is defined as:

$$SOC(t) = \frac{\theta_{max} - \theta_I(t)}{\theta_{max} - \theta_{min}}, \tag{4}$$

where the θ_{max} and θ_{min} are the maximum and minimum room temperature, respectively. In this study, the lower thermostat set point always has the same value as the minimum room temperature. The upper thermostat set point varies for different user preferences, and is set to the maximum room temperature only under the DR control.

The concept of equivalent SOC of the HVAC system is illustrated in Fig. 6. When the HVAC system is operating in the cooling mode, the maximum and minimum room temperature correspond to the equivalent SOC of 0% and

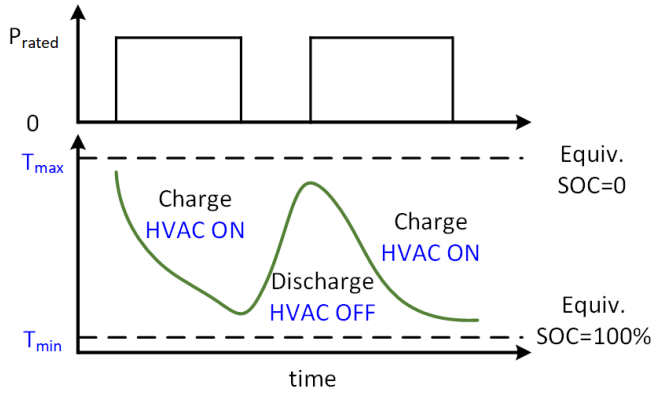

Fig. 6. The HVAC system as energy storage when cooling. The maximum and minimum room temperature correspond to the equivalent SOC of 0% and 100%, respectively. When the HVAC is ON, the room temperature decreases, as the equivalent of charging procedure of the BESS. On the contrary, the equivalent BESS "discharges" as the room temperature increases when the HVAC is OFF.

Algorithm 1: Calculate the energy storage capacity of the HVAC system

Set $\theta_O(t) = \theta_{O,F}$, $\theta_I(0) = \theta_{max}$, $m = 0$
while $\theta_I(m) > \theta_{min}$ **do**
  $m = m + 1$;
  $S(m) = 1$;
  calculated $\theta_I(m)$ in (2);
end
The energy capacity $E_C = P_H/COP \cdot \Delta t \cdot m$

100%, respectively. The room temperature increases due to the higher outside temperature when the HVAC is OFF, and this is the equivalent procedure of discharging the energy storage. When the HVAC is ON, the room temperature decreases in most of the normal cases and correspondingly, the equivalent SOC increases.

The energy capacity of a HVAC system is defined as the **input electricity** needed to change the room temperature from the maximum to the minimum with a fixed outside temperature. The pseudocode for the calculation is shown in Algorithm. 1. The energy capacity of the HVAC system for each house is calculated with its own set of parameters.

In this study, the outside temperature $\theta_{O,F}$ for the calculation of the HVAC energy capacity is fixed to 86F, as this is the average outdoor temperature in Glasglow, KY during the month of July when this DR study takes place [27]. The lower thermostat set point is fixed to 70F for all the HVAC systems.

The maximum room temperature θ_{max}, was selected to be 81F as this is the highest indoor temperature that results in a comfortable PMV rating under typical conditions for July as calculated by the online CBE Thermal Comfort Tool that follows ASHRAE Standard 55 [28]. A typical relative humidity of 54%, clothing level of 0.5 clo representing common indoor summer wear, an air speed of 0.1 m/s, and metabolic rate corresponding to sitting were used to verify that 81F results in

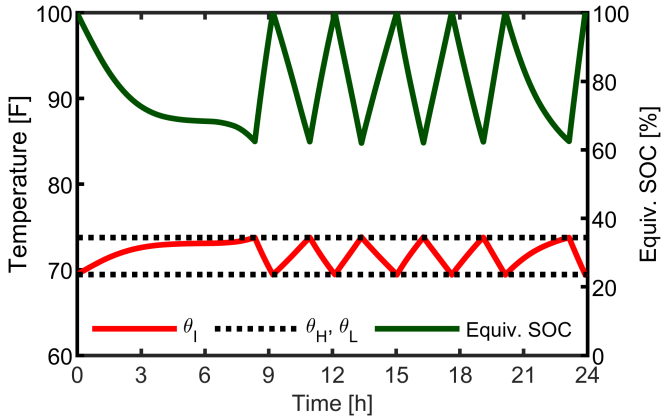

Fig. 7. Illustration of the relationship between room temperature and equivalent SOC based on the results shown in Fig. 3. The equivalent SOC was 100% when the room temperature reached the lower thermostat set point. The lowest equivalent SOC could be as high as 60% with a fixed upper thermostat set point, indicating the potential of deeper "discharge".

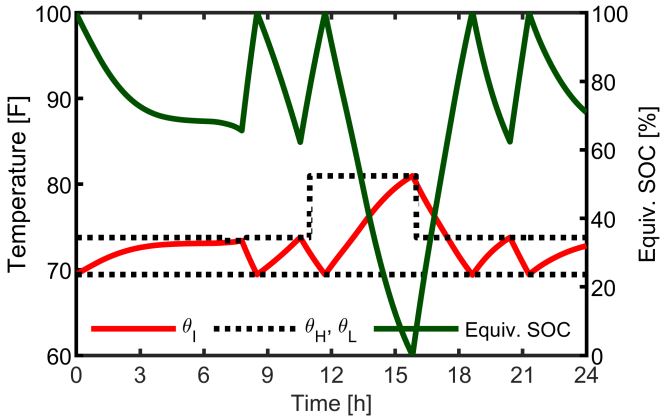

Fig. 8. The room temperature and equivalent SOC for the HVAC system with the sequential DR control. The equivalent SOC of the HVAC system could reach 0% by changing the upper thermostat set point to the maximum room temperature.

a PMV rating of 0.46 PMV. This is classified as acceptable as it is less than 0.5 PMV, meaning that 90% of people on average would be comfortable according to the ASHRAE Standards. The operative temperature was assumed equal to the indoor temperature or slightly lower, indicating the occupant would either be by a neutral or cool surface such as an interior wall out of sunlight or piece of furniture.

First in the equivalent energy storage study, the initial room temperature is set to the maximum and the HVAC is kept ON until the room temperature reaches the minimum. The required number of steps is recorded and used together with the heat transfer rate and the simulation resolution to calculate the energy capacity of the HVAC system. It is worth noting that the energy capacity is defined as the required **electricity**, therefore, the HVAC electric power, which is calculated as P_H/COP, is used for the calculation. The coefficient of performance (COP) and SEER are interchangeable.

The equivalent SOC of the HVAC system in the daily simulation example (Fig. 3) is shown in Fig. 7. In the morning, the HVAC was OFF and the room temperature increased until around 8:00, and the equivalent SOC decreased accordingly. When the HVAC was ON, the room temperature was decreased until it reached the lower thermostat set point. As a result, the equivalent SOC increased to 100%. The equivalent SOC did not drop below 60% in this example, indicating the potential to deepen "discharge" of the HVAC system through a control scheme.

The upper thermostat set point was set to the maximum room temperature during 11:00–16:00 for the DR control and the results are shown in Fig. 8. The equivalent SOC reached 0% as the room temperature became the maximum. The house could shed the HVAC power for a longer period of time by "discharging" the equivalent SOC to 0%.

TABLE II
THERMAL MODEL PARAMETERS DISTRIBUTED VALUES FOR THE LARGE AMOUNT OF RESIDENCES CONSIDERED

Parameter	Value (distribution)
Coefficient of thermal capacitance c_C	0.011 $^{kWh}/_{(^\circ C \cdot m^2)}$
Coefficient of heat transfer rate c_P	0.040 $^{kW}/_{m^2}$
Lower limit set point θ_L	70F
Upper limit set point θ_H	$\mathcal{U}(74F, 78F)$
Initial indoor temperature $\theta_I(0)$	$\mathcal{U}(70F, 74F)$
Thermal envelope area A_R	$\mathcal{N}(354, 200^2)$
Coefficient of thermal resistance c_R	$\mathcal{N}(350, 280^2)$

IV. Modeling of Aggregated HVAC Load

Every single residence in this study was modeled separately based on (2) and (3) with distinct sets of parameters. Each residential thermal model updates the indoor temperature dynamically considering the outside temperature, thermostat set points, and the DR signals. The aggregated HVAC power was calculated as:

$$P_A(t) = \frac{1}{SEER} \sum_{i=1}^{N} S^i(t) P_H^i, \tag{5}$$

where N is the total number of studied HVAC systems; P_H^i the heat transfer rate of house i in Btu/h.

The parameters of the thermal models across the community of residencies were selected to be either a specific constant value, normally distributed, or uniformly distributed (Table II). The values for some parameters of the residential thermal models were the same for all considered houses, i.e., the coefficients c_C and c_P, and the lower limit set point θ_L. The upper limit set points θ_H of all the houses without DR control were randomly generated to represent different user preference, noted as uniform distribution $\mathcal{U}(74F, 78F)$. The initial indoor temperatures were randomly generated within the lower limit of thermostat set point, 70F, and the lowest of the upper limit set points, 74F, noted as uniform distribution $\mathcal{U}(70F, 74F)$. Therefore, the initial temperature for all residences were bounded to the lower and upper set points.

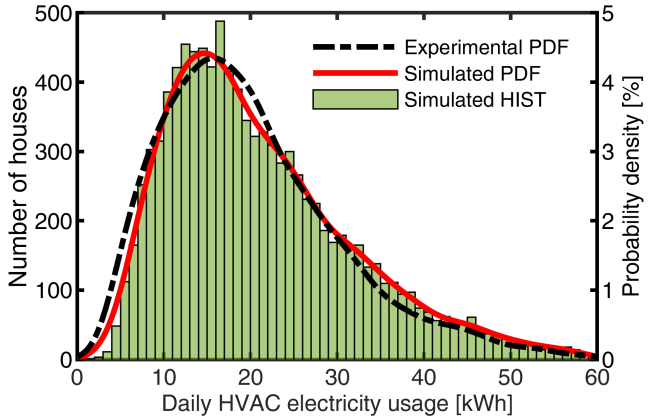

Fig. 9. The distribution of daily HVAC electricity usage on a typical summer day for 10,000 houses in a large community case study. The experimental probability density function (PDF) is estimated based on daily residential electricity usage from the SET project on the same day. The average electricity usage is approximately 21kWh based on the simulation.

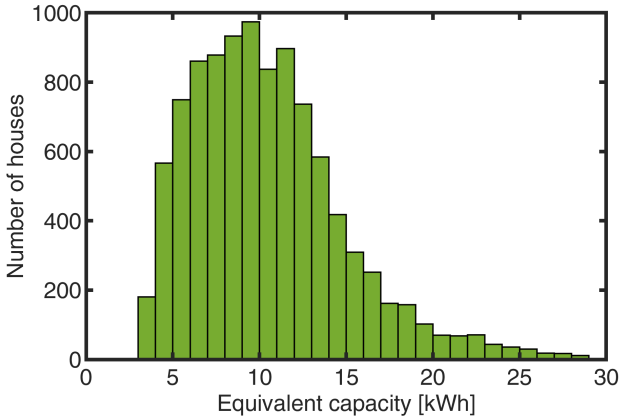

Fig. 10. The distribution of the energy storage capacities of the HVAC systems for 10,000 houses in a large community case study. The energy storage capacity of each residence was calculated separately according to its own set of parameters. The average equivalent energy capacity of the HVAC systems is approximately 11kWh.

The distribution types and parameters related to the house construction, A_R and c_R, were selected so that the simulation results matched the experimental data from the SET project. The A_R and c_R for the considered HVAC system models were subject to normal distributions and noted as $\boldsymbol{A_R} \sim \mathcal{N}(354, 200^2)$ and $\boldsymbol{c_R} \sim \mathcal{N}(350, 280^2)$. The daily electricity usages for each of the 10,000 HVAC systems in the example case were calculated and summarized into a histogram with a box size of 1kWh (Fig. 9). Both the experimental data and the simulation results were fitted to a nonparametric kernel-smoothing distribution and their probability density function (PDF) curves are presented in Fig. 9 as well. The comparison between the PDF curves of the simulated data and that of the experimental data demonstrates satisfactory results.

The energy storage capacity for each of the 10,000 HVAC systems was decided by their distinct sets of thermal model parameters, as described previously, and was calculated separately using the methods introduced in Algorithm 1. The results were summarized into a histogram (Fig. 10) to represent the community. The average energy storage capacity for the 10,000 HVAC systems is approximately 11kWh. Given that the typical energy consumption for HVAC systems is calculated at around 21kWh, the HVAC system as an energy storage device was charged/discharged approximately two rounds on the typical summer day in this study.

The simulated working status for the 10,000 participating HVAC systems without DR are shown in Fig. 11. In the early morning, even though the outdoor temperature was higher than the set point, not every HVAC turned ON due to the thermal inertia of the house. At approximately 9:00, many HVACs started to turn ON as the outdoor temperature increased quickly and the homes installation and shading could not prevent or slow heat transfer any longer.

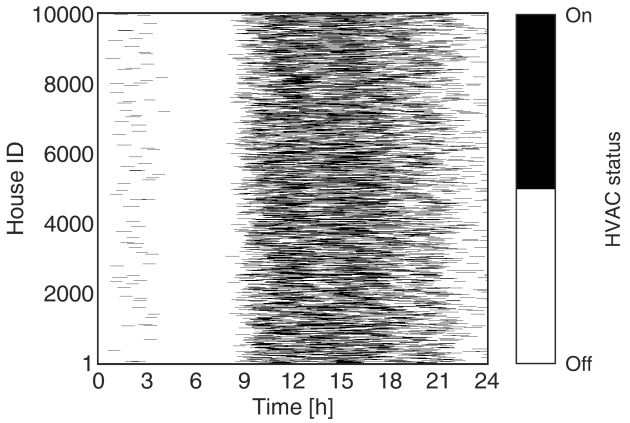

Fig. 11. The working status for the simulation of 10,000 participating HVAC systems without DR. Most of the HVAC systems started turning on around 9:00 due to the increase in outdoor temperature.

V. Optimal Control of the HVAC Systems

Two objectives were considered for VPP controls. The first is to reduce the peak power in the afternoon during 12:00 to 16:00:

$$\text{Minimize } P_{max} = \max\Big(P_A(t)\Big),\ t \in [12:00, 16:00]. \quad (6)$$

The second is to reduce the ramping rate of the aggregated HVAC power for the entire day:

$$\text{Minimize } \Delta P_{max} = \max\left(\frac{P_A(t+\Delta t) - P_A(t)}{\Delta t}\right), \quad t \in [0:00, 24:00]. \quad (7)$$

The objectives are realized by the central control system operated by the utility, which generates the DR signals for each residence according to one-day ahead weather forecasting data.

The DR control signals for each house include the upper limit thermostat set point, $\theta_{H,DR}$. When the DR event occurs in this study, the upper limit thermostat set point of the committed residence was changed to $\theta_{H,DR}$ = 73F for precooling and 81F for peak reduction.

In this paper, residences committed to the DR control will not overwrite the signals from the utility, for three reasons. First, residences committed to DR control enjoy financial rewards and are bounded by contract [29]. Second, under the DR control, the room temperature would still be kept comfortable for most of the users according to ASHRAE standards as described in previous section. Third, the DR signals from the utility will only be implemented at each house for short durations of time.

Houses are divided into multiple groups, and each group has its own scheduled time to apply the DR control by changing the upper limit thermostat set point. The HVAC systems in the same group apply the DR control for the same period of time. The next group of HVAC systems apply the DR control after a fixed time gap. The behavior of HVAC systems during a DR event is described as follows:

$$\begin{cases} \boldsymbol{\theta_H^1}(t_1) = \theta_{H,DR},\ t_1 \in [T_S, T_E] \\ \boldsymbol{\theta_H^2}(t_2) = \theta_{H,DR},\ t_2 \in [T_S + \Delta T_S, T_E + \Delta T_E] \\ ... \\ \boldsymbol{\theta_H^{n+1}}(t_{n+1}) = \theta_{H,DR},\ t_n \in [T_S + n\Delta T_S, T_E + n\Delta T_E], \end{cases} \tag{8}$$

where n is the group number; $\boldsymbol{\theta_H^n}$, the upper limit thermostat set points for all houses in group n; T_S and T_E are the times when the 1st group starts and ends the DR, respectively; ΔT_S, ΔT_E are the time gap between two groups to start and end DR, respectively.

In the example case, the 10,000 houses committed to DR control were divided into 100 groups, and each of their upper limit thermostat set points are shown in Fig. 12. The horizontal stripes indicate different customer preferences for indoor temperature. Two DR events were applied by changing the upper limit thermostat set points as shown by the blue and red vertical lines. The first DR event occurred in the morning as the upper limit thermostat set points of the first group were reduced to 73F from 7:00 to 8:00. Other groups followed sequentially by reducing their set points after a fixed time gap of 3 minutes between control adjustments, i.e., group two 7:03–8:03, group three 7:06–8:06, etc. Since there are 100 groups, the last batch of residences were precooled from 12:00–13:00.

The second DR event occurred in the afternoon for peak reduction between 12:00 and 16:00 (Fig. 12). Starting from 11:00, the first group of the HVAC systems increased the upper limit thermostat set point to 81F. Other groups increased their set points at a fixed time gap of 3 minutes, in a sequential way. The first group reverted to the original set points at 16:00 and other groups followed with a fixed time gap of 2 minutes, in the proposed staggered pattern. The time gaps to implement

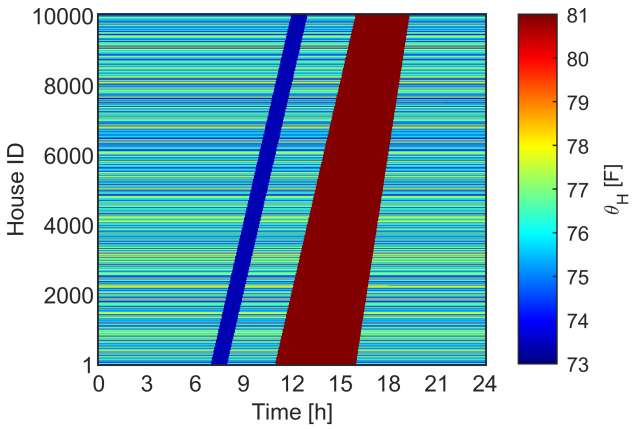

Fig. 12. The upper limit thermostat set points for all the 10,000 HVAC systems within the proposed sequential DR control. The different set points indicate the various user preferences. The values were set to low in the morning for precooling, and set to high in the afternoon to reduce the peak, both in a sequential way.

the DR control and to resume the original set point of the user are intentionally different to demonstrate the flexibility of the proposed sequential control.

It is worth noting that the DR signal for precooling and peak reduction in this case overlapped between 11:00 and 13:00, for three reasons. First, the precooling was for the reduction of ramping rate. Therefore, if the duration of precooling DR is short, the ramping rate would be large as many HVAC systems are turned ON in a short period of time. Second, if the precooling starts very early, the natural process of heat transferring from outside to the residence will start before the temperature outside has risen to an uncomfortable level, leading to unnecessary additional electricity usage. Third, the overlapping structure provides a buffer time to avoid sudden drops in the aggregated HVAC power.

VI. Control Results and Analysis

The time step for the simulations in this section is 1-minute. The simulation results were integrated to 15-minute resolution, which is the conventional time interval used by utilities in metering, to calculate the ramping rate. When 100% of the 10,000 residences participated in the DR control, the working status of the HVAC systems are shown in Fig. 13. The proposed sequential DR control resulted in three clear stripes of HVAC state changes, namely, the one starting at 7:00, the one at around noon, and the one starting at 16:00. The HVAC systems were turned ON and OFF in a sequential way in order to avoid sudden changes of the aggregated power when the thermostat set points were changed by the DR control.

The same 10,000 HVAC systems were simulated using the same outdoor temperature both with and without DR control. The outdoor temperature and average indoor temperatures for both cases are shown in Fig. 14. Also shown are the simulated indoor temperatures of individual houses with the DR control. In the study, the lower limit thermostat set point was fixed to 70F for all the houses. The upper limit thermostat set points for

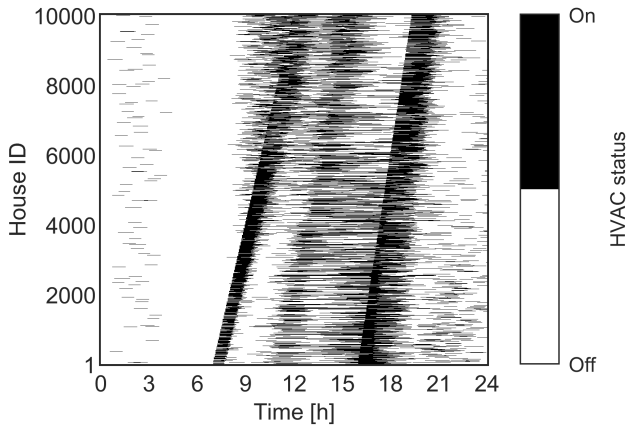

Fig. 13. The working status for the simulation of 10,000 HVAC systems in a DR study with centralized controls. HVAC systems were turned ON/OFF in a sequential way, reducing the ramping rate and the peak load.

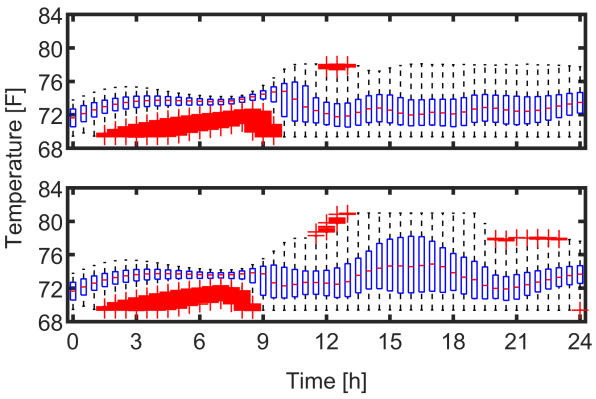

Fig. 15. The indoor temperature variations of all 10,000 residences (top: without DR control, bottom: with DR control). The effect of precooling can be spotted around 9:00, and the effect of peak reduction can be observed in the afternoon.

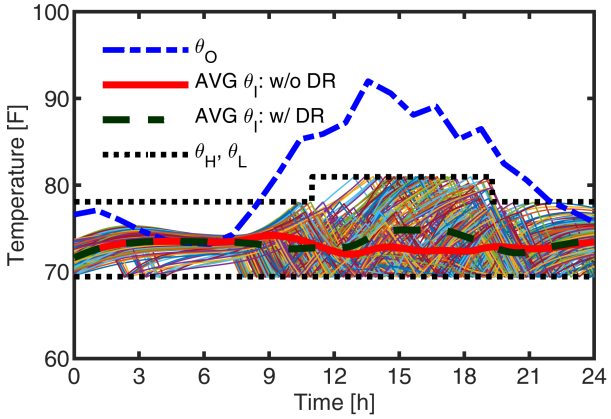

Fig. 14. The outdoor temperature and average indoor temperatures of the 10,000 simulated HVAC systems. For the DR program, indoor temperature was allowed to be higher but still acceptable according to ASHRAE standards.

all the 10,000 houses were uniformly distributed in the range of [74F, 78F] in order to represent various user preferences.

When the DR signal arrived in the afternoon, the upper limit thermostat set points for the batch of houses under control were set to 81F. In Fig. 14, only the highest value of the upper limit thermostat set point from all the residences at each time step was plotted. For example, when there was no DR signals, the upper limit thermostat set points for all houses are between 74F and 78F ($\theta_H \in [74F, 78F]$). When there was DR signal for precooling in the morning, $\theta_H \in [73F, 78F]$, and where the DR signal was for peak reduction, $\theta_H \in [74F, 81F]$. The θ_H in the plot was 81F when there was DR control for peak reduction in the afternoon, and 78F for other durations.

The selection of the maximum allowed indoor temperature, which is 81F for the illustrated example, is based on a combination of human comfort regulations, as per ASHRAE Standard 55-2017, and user behavior preferences, as expressed through enrollment in different DR schemes that trade comfort controls versus unitary electricity cost [13]. It should be noted that the average temperature for all homes does not exceed 75F at any time and that only very few homes, which selected a minimum electricity cost DR program option, reach the 81F maximum temperature after 17:00, and even then, only for a very short duration of time.

The indoor temperature of all 10,000 residences were presented with a sampling frequency of 30-minute in boxplot (Fig. 15). When the residences were precooled (bottom), their indoor temperatures were lower at around 9:00, which allowed more HVAC systems to stay OFF and reduced the ramping rate. In the afternoon, the maximum indoor temperature of some residences reached 81F under the DR control, which was the highest temperature still acceptable for most users under the conditions explained in the previous section. Even so, given any time point, the indoor temperature for 75% of the residences was no more than 78F, which appeared at 16:00.

The equivalent SOC for the houses without DR is shown in Fig. 16. The HVAC systems operated as energy storage devices were "discharged" at different levels due to the various upper limit thermostat set points. None of the houses were "discharged" thoroughly to 0% without DR control.

Some of the HVAC systems were thoroughly "discharged" to 0% at the critical hours due to the DR control, as shown in Fig. 17. The sequential control implemented in this study avoided "discharging" all the HVAC systems to 0% at the same time, in order to avoid the large rebound ramping rate afterwards. The aggregated SOC started to decrease from 12:00, indicating the equivalent "discharging" process as use of stored energy. This demonstrates that the HVAC systems could operate comparably with the batteries.

The proposed sequential DR control strategy is exemplified by this study that successfully results in a very large reduction of the peak power from 12:00 to 16:00 through temporarily allowing higher temperatures inside the participating homes. The indoor temperatures in Fig. 14 were the results for 100% participation of 10,000 residences on an example summer day.

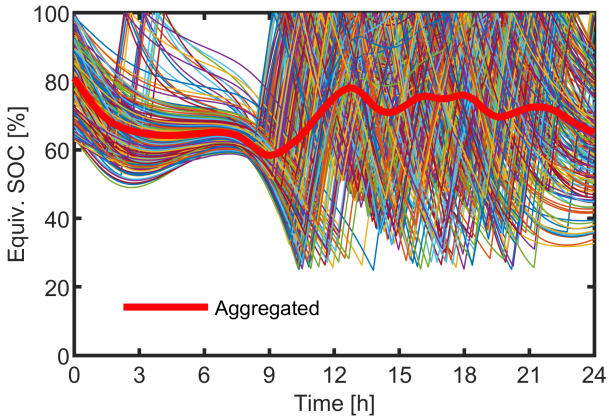

Fig. 16. Simulation results of the equivalent SOC for the 10,000 HVAC systems studied without DR control. None of the houses were "discharged" thoroughly during the peak hour.

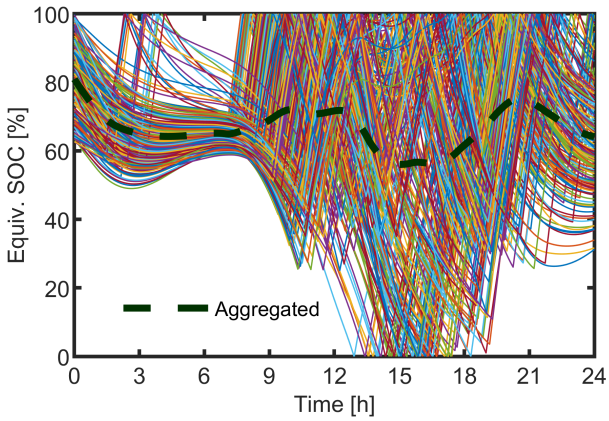

Fig. 17. Simulation results of the equivalent SOC for the 10,000 HVAC systems studied with DR control. Houses were fully "discharged" as the equivalent SOC reached 0% at different period of time. The aggregated equivalent SOC did not reach 0% because not all the houses were fully "discharged" at the same time. The sequential DR control was implemented to avoid the large rebound ramping rate afterwards.

The corresponding aggregated HVAC power and equivalent SOC are shown in Figs. 18 and 19 with different residence participation for the same day. The simulation results for different residence participation levels are summarized in Table III where it can be seen that the ramping rate and total daily electricity usage are decreased with more participation. The residences participating in the simulated DR program were selected based on their house ID in ascending sequence in this study.

The aggregated HVAC power from Fig. 18 shows that, under normal operation without DR controls, the ramping rate around 8:00 was large due to many HVAC systems starting around the same time, and the peak power from 12:00 to 16:00 was high due to high outdoor temperature. The ramping rate, peak power in the afternoon, and the total daily HVAC electricity were reduced under the proposed sequential control, even with low residence participation. When the participation

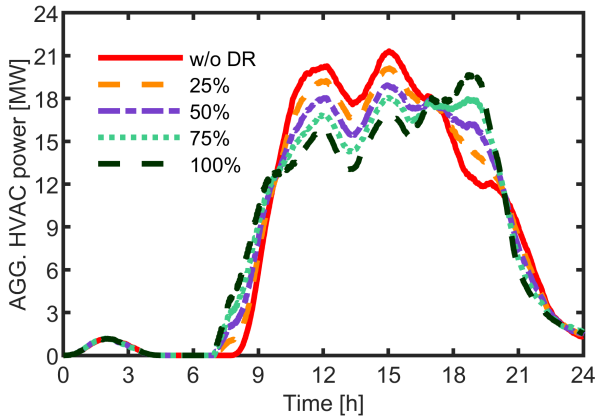

Fig. 18. Simulation results of aggregated HVAC power for the 10,000 houses studied on 7/14 with different residence participation. The legends stand for the residence participation in DR control. Detailed simulation results are summarized in Table III.

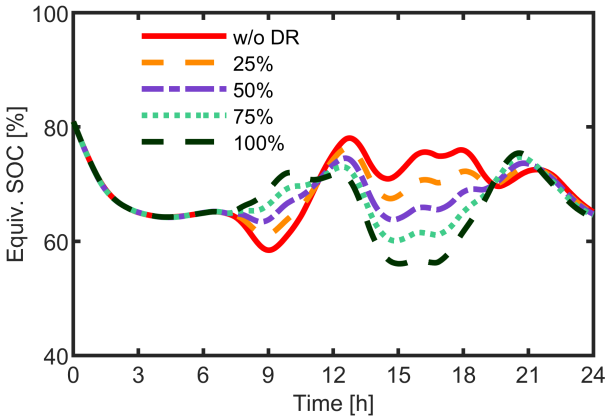

Fig. 19. Simulation results of the aggregated equivalent SOC for the 10,000 HVAC systems studied on 7/14 with different residence participation.

rate is high, e.g., 100%, the peak power period for the DR case was shifted to a later time as a consequence of indoor temperature recovery, and in addition, the ramping rate was greatly reduced.

The aggregated equivalent SOC of the 10,000 HVAC systems shown in Fig. 19 demonstrates the effectiveness of the proposed sequential DR control scheme, which provided benefit to the utility as described while still resulting in a near 65% aggregated equivalent SOC as was the same as on

TABLE III
SUMMARY OF SIMULATION RESULTS FOR DIFFERENT RESIDENCE PARTICIPATION

Participation [%]	P_{max} [MW]	ΔP_{max} [MW/15-min]	Daily Elec. [MWh]
0 (w/o DR)	21.3	36.2	213
25	20.1	31.6	211
50	18.9	29.7	208
75	18.1	25.3	206
100	16.8	23.4	203

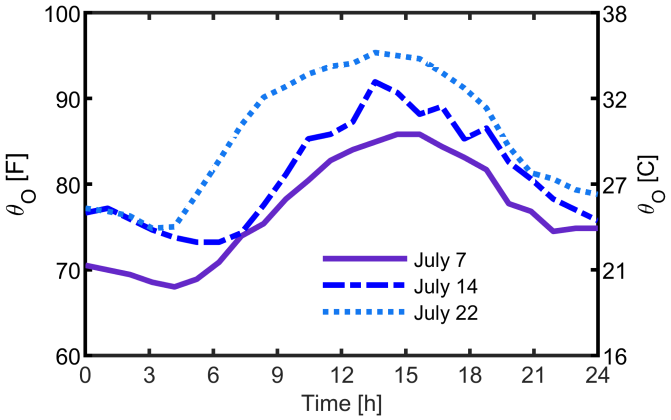

Fig. 20. Outside temperature of example days selected from the experimental data from Glasgow, KY, in the year of 2017. The proposed sequential control was tested on the days with high outside temperatures when the HVAC systems tend to have high cooling power demand.

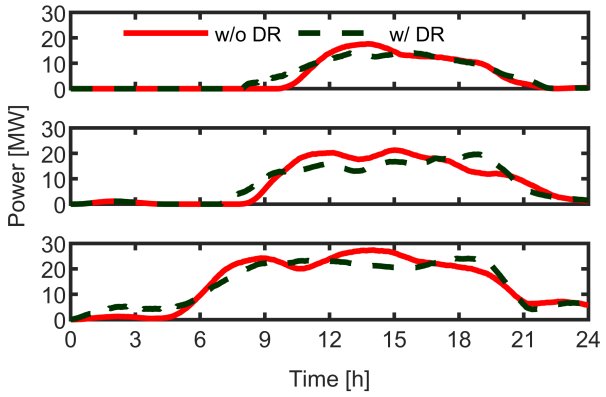

Fig. 21. Simulation results of aggregated HVAC power for the 10,000 houses studied on different hot days (top to bottom: 7/7, 7/14, 7/22). The ramping rate in the morning, as well as the peak power in the afternoon from 12:00 to 16:00 were reduced. Detailed simulation results are summarized in Table IV.

the day before DR was applied. Another important note is that the total energy storage capacity for the 10,000 residences was fixed because the energy capacity of each HVAC system was fixed, as explained in Section III. The equivalent precharging process, which started from 7:00, avoided significant power draw at 12:00 and large ramping rate starting from 9:00. The peak power in the afternoon from 12:00 to 16:00 was reduced by the equivalent discharging process. The proposed sequential DR control managed to postpone the equivalent charging process to 18:00.

The outside temperature is stochastic and therefore, the DR control scheme for the simulation of aggregated HVAC power as an energy storage resource was repeated on two additional different hot days in the summer (Fig. 20). In this paper, the proposed sequential control was demonstrated in the hot days because the fuel for space cooling is 100% electricity, and the peak reduction is only needed when the HVAC systems have high power. The proposed sequential control was not shown for cold days as some of the residences might use fuels other than electricity for heating [30]. Therefore, the results of the sequential control for cooling are directly related to the number of residences participating in the DR control, while for heating, the portion of electricity-heating houses must be considered.

The simulation results for different summer days are presented in Fig. 21 and summarized in Table IV. In this comparison, the DR control participation was considered 100%. The case study for w/o DR and 100% participation in Fig. 18 and Table III is referred as "Day: 7/14" (middle).

The case "Day: 7/7" (top) represents a slightly cooler summer day. The proposed sequential control reduced the already low ramping rate by precooling and peak power by turning ON the HVAC systems in batches during a longer time span. The total daily electricity usage was increased by 2% under the proposed DR control due to the precooling. This happened because lower temperature in the morning resulted in more heat transferring into the houses.

TABLE IV
SUMMARY OF SIMULATION RESULTS FOR DIFFERENT DAYS

Day	Participation [%]	P_{max} [MW]	ΔP_{max} [MW/15-min]	Daily Elec. [MWh]
7/7	0 (w/o DR)	17.7	30.7	125
	100%	14.2	17.9	128
7/14	0 (w/o DR)	21.3	36.2	213
	100%	16.8	23.4	203
7/22	0 (w/o DR)	27.4	34.4	349
	100%	23.0	22.3	347

The case "Day: 7/22" (bottom) represents a very hot day when the ramping rate and peak power of the aggregated HVAC power without DR control were high. The proposed sequential control reduced the maximum ramping rate by 35% and the peak power during 12:00 to 16:00 by 16% while the total daily electricity maintained nearly the same.

The aggregated equivalent SOC of the 10,000 residences for the three different days are shown in Fig. 22. For the 7/7 case (top), the equivalent SOC was maintained higher starting from 9:00 because of the precooling to avoid high ramping rate for "charging" starting from around 10:30. For the 7/14 case (middle), the precooling started from around 7:30, avoiding high ramping rate starting from around 9:00. For the 7/22 case (bottom), the precooling moved the equivalent "charging" process from 6:00 to early morning, reducing the ramping rate. For all the cases, the lower equivalent SOCs in the afternoon demonstrate the HVAC system can "discharge" as energy storage to reduce the peak power.

VII. CONCLUSION

This paper proposes an aggregation technique for the modeling of HVAC systems in large communities that is based on the robotic house managed by the Tennessee Valley Authority (TVA). This house is considered typical by their analysis and emulates human behavior with the operation schedules for the appliances inside. The proposed aggregation technique

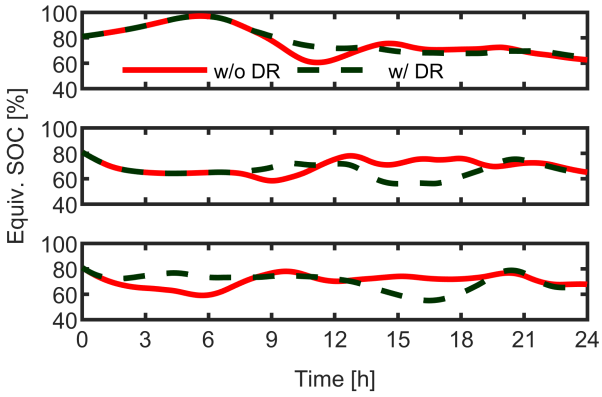

Fig. 22. Simulation results of the aggregated equivalent SOC for the 10,000 HVAC systems on different hot days (top to bottom: 7/7, 7/14, 7/22). With the DR control, the equivalent precharging process in the morning reduced the ramping rate. The HVAC systems as energy storage discharged deeper in the afternoon under DR control and reduced the peak power.

employs a realistic distribution of parameters and loads, which were derived with data from the SET Project, one of the largest smart grid field demonstrators in rural America. The example building model and its equivalent circuit parameter values provide a useful reference that is suitable for Virtual Power Plant (VPP) and demand response (DR) studies of HVAC systems in large residential distribution systems.

Also proposed is a VPP sequential control scheme that temporarily allows higher indoor temperatures up to values that are still considered acceptable for typical preferences and standard regulations of human comfort. The results based on 10,000 HVAC systems show that, on a very hot summer day, when the DR participation was 100%, the peak power in the afternoon and the ramping rate were reduced by approximately 16% and 35%, respectively while the daily energy usage was almost the same. This paper also develops an equivalent energy storage model for HVAC systems and demonstrates that HVAC systems can be controlled in a charging/discharging procedure similar to a typical battery at both individual and aggregated levels.

VIII. Acknowledgment

The support of the Tennessee Valley Authority (TVA) and of University of Kentucky, the L. Stanley Pigman endowment is gratefully acknowledged.

References

[1] "Residential energy consumption survey (RECS)," https://www.eia.gov/consumption/residential/index.php, accessed: 2020-06-29.

[2] M. Hu, F. Xiao, and L. Wang, "Investigation of demand response potentials of residential air conditioners in smart grids using grey-box room thermal model," *Applied energy*, vol. 207, pp. 324–335, 2017.

[3] M. Hu and F. Xiao, "Price-responsive model-based optimal demand response control of inverter air conditioners using genetic algorithm," *Applied energy*, vol. 219, pp. 151–164, 2018.

[4] W. Zhang, J. Lian, C. Chang, and K. Kalsi, "Aggregated modeling and control of air conditioning loads for demand response," *IEEE Transactions on Power Systems*, vol. 28, no. 4, pp. 4655–4664, 2013.

[5] G. Goddard, J. Klose, and S. Backhaus, "Model development and identification for fast demand response in commercial hvac systems," *IEEE Transactions on Smart Grid*, vol. 5, no. 4, pp. 2084–2092, 2014.

[6] X. Zhang, M. Cai, M. Pipattanasomporn, and S. Rahman, "A power disaggregation approach to identify power-temperature models of hvac units," in *2018 IEEE International Smart Cities Conference (ISC2)*, 2018, pp. 1–6.

[7] D. T. Vedullapalli, R. Hadidi, and B. Schroeder, "Optimal demand response in a building by battery and hvac scheduling using model predictive control," in *2019 IEEE/IAS 55th Industrial and Commercial Power Systems Technical Conference (I CPS)*, 2019, pp. 1–6.

[8] M. Cai, S. Ramdaspalli, M. Pipattanasomporn, S. Rahman, A. Malekpour, and S. R. Kothandaraman, "Impact of hvac set point adjustment on energy savings and peak load reductions in buildings," in *2018 IEEE International Smart Cities Conference (ISC2)*, 2018, pp. 1–6.

[9] Q. Shi, C.-F. Chen, A. Mammoli, and F. Li, "Estimating the profile of incentive-based demand response (IBDR) by integrating technical models and social-behavioral factors," *IEEE Transactions on Smart Grid*, vol. 11, no. 1, pp. 171–183, 2019.

[10] J. H. Yoon, R. Baldick, and A. Novoselac, "Dynamic demand response controller based on real-time retail price for residential buildings," *IEEE Transactions on Smart Grid*, vol. 5, no. 1, pp. 121–129, 2014.

[11] M. Tavakkoli, S. Fattaheian-Dehkordi, M. Pourakbari-Kasmaei, M. Liski, and M. Lehtonen, "Bonus-based demand response using stackelberg game approach for residential end-users equipped with hvac system," *IEEE Transactions on Sustainable Energy*, vol. 12, no. 1, pp. 234–249, 2021.

[12] A. Taşcıkaraoğlu, N. G. Paterakis, O. Erdinç, and J. P. Catalao, "Combining the flexibility from shared energy storage systems and dlc-based demand response of hvac units for distribution system operation enhancement," *IEEE Transactions on Sustainable Energy*, vol. 10, no. 1, pp. 137–148, 2018.

[13] American National Standards Institute and American Society of Heating, Refrigerating and Air-Conditioning Engineers, ANSI/ASHRAE *Standard 55-2017 Thermal environmental conditions for human occupancy*. American Society of Heating, Refrigerating and Air-Conditioning Engineers (ASHRAE), 2017.

[14] J. Dong, M. Starke, B. Cui, J. Munk, E. Tsybina, C. Winstead, Y. S. Xue, M. Olama, and T. Kuruganti, "Battery equivalent model for residential hvac," in *2020 IEEE Power & Energy Society General Meeting (PESGM)*. IEEE, 2020, pp. 1–5.

[15] J. Wang, S. Huang, D. Wu, and N. Lu, "Operating a commercial building hvac load as a virtual battery through airflow control," *IEEE Transactions on Sustainable Energy*, vol. 12, no. 1, pp. 158–168, 2020.

[16] N. S. Raman and P. Barooah, "On the round-trip efficiency of an hvac-based virtual battery," *IEEE Transactions on Smart Grid*, vol. 11, no. 1, pp. 403–410, 2019.

[17] S. Ahmad Hamidi, D. M. Ionel, and A. Nasiri, "Modeling and management of batteries and ultracapacitors for renewable energy support in electric power systems–an overview," *Electric Power Components and Systems*, vol. 43, no. 12, pp. 1434–1452, 2015.

[18] D. Madjidian, M. Roozbehani, and M. A. Dahleh, "Battery capacity of deferrable energy demand," in *2016 IEEE 55th Conference on Decision and Control (CDC)*. IEEE, 2016, pp. 4220–4225.

[19] H. Gong, V. Rallabandi, M. L. McIntyre, E. Hossain, and D. M. Ionel, "Peak reduction and long term load forecasting for large residential communities including smart homes with energy storage," *IEEE Access*, vol. 9, pp. 19 345–19 355, 2021.

[20] H. Gong, V. Rallabandi, D. M. Ionel, D. Colliver, S. Duerr, and C. Ababei, "Dynamic modeling and optimal design for net zero energy houses including hybrid electric and thermal energy storage," *IEEE Transactions on Industry Applications*, vol. 56, no. 4, pp. 4102–4113, 2020.

[21] B. Cui, J. Dong, J. D. Munk, N. Mao, and T. Kuruganti, "A simplified regression building thermal modelling method for detached two-floor house in us," Oak Ridge National Lab.(ORNL), Oak Ridge, TN (United States), Tech. Rep., 2018.

[22] H. Gong, E. S. Jones, and D. M. Ionel, "An aggregated and equivalent home model for power system studies with examples of building insulation and hvac control improvements," in *2020 IEEE Power & Energy Society General Meeting (PESGM)*. IEEE, 2020, pp. 1–4.

[23] X. Chen, Q. Hu, Q. Shi, X. Quan, Z. Wu, and F. Li, "Residential hvac aggregation based on risk-averse multi-armed bandit learning for

secondary frequency regulation," *Journal of Modern Power Systems and Clean Energy*, vol. 8, no. 6, pp. 1160–1167, 2020.
[24] H. Gong, E. S. Jones, R. E. Alden, A. G. Frye, D. Colliver, and D. M. Ionel, "Demand response of hvacs in large residential communities based on experimental developments," in *2020 IEEE Energy Conversion Congress and Exposition (ECCE)*. IEEE, 2020, pp. 4545–4548.
[25] H. Gong, V. Rallabandi, M. L. McIntyre, and D. M. Ionel, "On the optimal energy controls for large scale residential communities including smart homes," in *2019 IEEE Energy Conversion Congress and Exposition (ECCE)*, Baltimore, MD, USA, 2019, pp. 503–507.
[26] D. S. Callaway, "Tapping the energy storage potential in electric loads to deliver load following and regulation, with application to wind energy," *Energy Conversion and Management*, vol. 50, no. 5, pp. 1389–1400, 2009.
[27] Weather Spark, "Average Weather in July in Glasglow Kentucky, United States," https://weatherspark.com/m/15163/7/Average-Weather-in-July-in-Glasgow-Kentucky-United-States#Sections-Temperature, accessed: 2021-04-15.
[28] F. Tartarini, S. Schiavon, T. Cheung, and T. Hoyt, "CBE thermal comfort tool: Online tool for thermal comfort calculations and visualizations," *SoftwareX*, vol. 12, p. 100563, 2020.
[29] X. Xu, C.-f. Chen, X. Zhu, and Q. Hu, "Promoting acceptance of direct load control programs in the United States: Financial incentive versus control option," *Energy*, vol. 147, pp. 1278–1287, 2018.
[30] U.S. Energy Information Administration (EIA), "Residential Energy Consumption Survey (RECS)," https://www.eia.gov/consumption/residential/data/2015/hc/php/hc6.1.php, accessed: 2021-07-28.

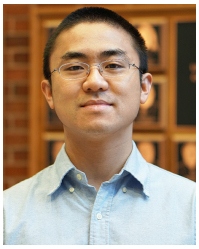

Huangjie Gong (S'18) received the B.Eng. degree in automation from Harbin Engineering University, Harbin, China, in 2013 and the M.S. degree in control theory and control engineering from Southwest Jiaotong University, Chengdu, China, in 2016. Since 2017 he is a Ph.D. student in the SPARK Laboratory, ECE Department at University of Kentucky, Lexington, KY, where he has been working on research projects sponsored by DOE, NSF, Electric Power Research Institute (EPRI), industry and utilities. He is the main developer of a large-scale co-simulation software framework for energy in buildings and power flow in electric distribution systems. In 2021, he was a graduate student intern with the National Renewable Energy Laboratory (NREL). He is an executive committee member for the joint student chapter at UK and a member of PES renewable energy generation subcommittee. His research interests include renewable energy integration, modeling and control of energy storage, batteries, water heaters, HVAC systems, EV, net zero energy (NZE) buildings, and microgrids.

Evan S. Jones received B.S. degrees in electrical engineering and computer engineering with a minor in computer science from the University of Kentucky (UK), Lexington, Kentucky, USA in 2019. He is currently a PhD student in the SPARK Laboratory and a U.S. Department of Education GAANN Ph.D. Fellow. During his undergraduate studies, he was an L. Stanley Pigman Scholar, an IEEE PES Plus Scholarship recipient, and a student engineer for the EKPC utility. At UK, he worked on research projects sponsored by the Department of Energy (DOE), Electric Power Research Institute (EPRI), and the TVA and LG&E and KU utilities. He served as the Vice Chair for the joint student chapter of IEEE PES and IAS at UK. His research interests include building energy models (BEMs), virtual power plants (VPPs), electric power systems, and renewable energy generation and integration.

Rosemary E. Alden received in 2021 her B.S. in electrical engineering from the University of Kentucky, Lexington, Kentucky, USA, where she is currently a PhD student in the SPARK Lab. During her undergraduate studies, she was an L. Stanley Pigman Scholar and an IEEE PES Plus Scholarship recipient. She is now a National Science Foundation (NSF) Graduate Research Fellow. She was an intern with the Electric Power Research Institute (EPRI) and with the National Renewable Energy Laboratory (NREL). She has been serving as the inaugural chair for the joint student chapter of IEEE PES and IAS at UK. Her research interests include machine learning, electric load forecasting, smart buildings and grid, and power system grid analysis for renewable energy integration.

Drew Frye leads the development of TVA's Electric Vehicle (EV) programs. Drew coordinates program and partnership development with EV stakeholders and regional Local Power Companies to remove the market barriers slowing EV adoption in the Tennessee Valley. Initiatives include charging infrastructure availability, consumer awareness and education, supportive policy development and vehicle availability and choice. Drew's team is leading the "Fast Charge Network" program to deploy fast charging stations along major travel corridors across TVA's service territory in partnership with Local Power Companies and state agencies.

Previously, Drew served in TVA's research organization for ten years with focuses on various grid edge technologies such as Electric Transportation. He is an advisor to the Electric Power Research Institute where he interfaces with active utilities from across the country.

Drew has a Master of Science degree in Power Systems Engineering from UT Chattanooga and a Bachelor of Science degree in Mechanical Engineering from the University of Tennessee. He lives in Chattanooga, TN with his wife Lauren, six year old daughter Lucie and they are expecting another little girl this summer.

Donald Colliver received the B.S. and M.S. degrees in Agricultural Engineering at University of Kentucky and the Ph.D. degree in Agricultural Engineering at Purdue University.

He is currently Professor and Director of Graduate Studies in the Biosystems Engineering Department at the University of Kentucky and Director of the Kentucky Industrial Assessment Center. He has conducted and managed extensive research in energy usage in residential and commercial buildings and industrial facilities, solar energy, air infiltration and ventilation, building codes, and the analysis of climatological data for determination of design weather conditions. He is a Fellow of the American Society of Heating, Refrigerating and Air- Conditioning Engineers (ASHRAE) served as its President in 2002-2003.

Dan M. Ionel (M'91–SM'01–F'13) received the M.Eng. and Ph.D. degrees in electrical engineering from the Polytechnic University of Bucharest, Bucharest, Romania. His doctoral program included a Leverhulme Visiting Fellowship with the University of Bath, Bath, U.K and he later was a Post-doctoral Researcher with the SPEED Laboratory, University of Glasgow, Glasgow, U.K.

Dr. Ionel is a professor of electrical engineering and the L. Stanley Pigman Chair in Power with the University of Kentucky, Lexington, KY, USA, where he is also the Director of the Power and Energy Institute of Kentucky and of the SPARK Laboratory. He previously worked in industry for more than 20 years. Dr. Ionel's current research group projects on smart grid and buildings, and integration of distributed renewable energy resources and energy storage in the electric power systems are sponsored by NSF, DOE, industry and utilities. He published more than 200 technical papers, including some that received IEEE awards, was granted more than 30 patents, and is co-author and co-editor of the book "Renewable Energy Devices and Systems – Simulations with MATLAB and ANSYS", CRC Press.

Dr. Ionel received the IEEE PES Veinott Award, was the Inaugural Chair of the IEEE IAS Renewable and Sustainable Energy Conversion Systems Committee, an Editor for the IEEE TRANSACTIONS ON SUSTAINABLE ENERGY, and the Technical Program Chair for IEEE ECCE 2016. He is the Editor in-Chief for the Electric Power Components and Systems Journal, and the Chair of the Steering Committee for IEEE IEMDC.